https://doi.org/10.5194/acp-2020-34
Preprint. Discussion started: 20 January 2020

Atmospheric Chemistry and Physics Discussions

Partitioning of hydrogen peroxide in gas-liquid and gas-aerosol phases

Xiaoning Xuan[1], Zhongming Chen[1], Yiwei Gong[1], Hengqing Shen[1], and Shiyi Chen[1]

[1]State Key Laboratory of Environmental Simulation and Pollution Control, College of Environmental Sciences and Engineering, Peking University, Beijing, 100871, China

Correspondence to: Zhongming Chen (zmchen@pku.edu.cn)

Abstract. Hydrogen peroxide (H_2O_2) is a vital oxidant in the atmosphere and plays critical roles in the oxidation chemistry of both liquid and aerosol phases. The partitioning of H_2O_2 between the gas and liquid phase or the aerosol phase could affect its abundance in these condensed phases and eventually the formation of secondary components. However, the partitioning processes of H_2O_2 in gas-liquid and gas-aerosol phases are still unclear, especially in the ambient atmosphere. In this study, field observations of gas-, liquid-, and aerosol-phase H_2O_2 were carried out in the urban atmosphere of Beijing during the summer and winter of 2018. The effective field-derived mean value of Henry's law constant (H_A^m, 2.1×10^5 M atm^{-1}) was 2.5 times that of the theoretical value in pure water (H_A^t, 8.4×10^4 M atm^{-1}) at 298 ± 2 K. The effective derived gas-aerosol partitioning coefficient (K_P^m, 3.8×10^{-3} m^3 μg^{-1}) was four orders of magnitude higher on average than the theoretical value (K_P^t, 2.8×10^{-7} m^3 μg^{-1}) at 270 ± 4 K. The partitioning of H_2O_2 in the gas-liquid and gas-aerosol phases in the ambient atmosphere does not only obey Henry's law or Pankow's absorptive partitioning theory but is also influenced by certain physical and chemical reactions. The average concentration of liquid-phase H_2O_2 in rainwater during summer was 44.12 ± 26.49 μM. In three-quarters of the collected rain samples, the measured H_2O_2 was greater than the predicted value in pure water calculated by Henry's law. In these samples, 46 % of the measured H_2O_2 was from gas-phase partitioning, and most of the rest may have come from residual H_2O_2 in raindrops. In winter, the level of aerosol-phase H_2O_2 was 0.093 ± 0.085 ng μg^{-1}, which was much higher than the predicted value based on Pankow's absorptive partitioning theory. Almost all aerosol-phase H_2O_2 was not from the partitioning of the gas phase. The decomposition/hydrolysis of aerosol-phase organic peroxides could be responsible for 32 % of aerosol-phase H_2O_2 formation at the maximum rate of 3.65 ng μg^{-1}. Furthermore, the heterogeneous uptake of H_2O_2 on aerosols contributed to less than 0.5 %.

1 Introduction

Hydrogen peroxide (H_2O_2), regarded as a significant oxidant in the liquid and aerosol phases, is of great significance to the oxidation capacity in these phases (Reeves and Penkett, 2003). In addition to its direct effect as an oxidant, H_2O_2 also serves as the temporary reservoir species that cycles and redistributes the HO_x radical (Lee et al., 2000; Tong et al., 2016; Crowley et al., 2018). Owing to larger solubility in water (O'Sullivan et al., 1996) and larger reaction rate with reduced substances

https://doi.org/10.5194/acp-2020-34
Preprint. Discussion started: 20 January 2020


Atmospheric Chemistry and Physics Discussions

(Seinfeld and Pandis, 2006), H_2O_2 plays a vital part in the fast formation of sulfate (SO_4^{2-}) and fine particles ($PM_{2.5}$) during heavy haze episodes (Stein and Saylor, 2012; Qin et al., 2018; Ye et al., 2018; Liu et al., 2020). Furthermore, H_2O_2, as a typical reactive oxygen species (ROS), has adverse health effects and contributes to incidences of lung cancer, asthma, and cardiopulmonary disease (Gurgueira et al., 2002; Zhao et al., 2011; Campbell et al., 2019).

As is well known, H_2O_2 in the liquid and aerosol phases is generally assumed to originate from the partitioning of gas-phase H_2O_2. Furthermore, the partitioning of H_2O_2 between the gas-liquid and gas-aerosol phases is expected to obey Henry's law and Pankow's absorptive partitioning theory, respectively. Studies of the partitioning process of H_2O_2 contribute to a clearer understanding of the sources of limiting oxidants and estimates of the contribution to sulfate formation in the liquid and aerosol phases. In this study, we define the field-derived ratios of the measured levels of gas-to-liquid and gas-to-aerosol phases as the effective Henry's law constant and the gas-aerosol partitioning coefficient, respectively.

However, it is interesting that the predicted liquid-phase concentration of H_2O_2 in rainwater using Henry's law was not sufficient to account for the measured level, and a large amount of liquid-phase H_2O_2 was produced from other reactions (Liang et al., 2013). Chung et al. (2005) demonstrated that the "salting-in" effect could as much as double the solubility of H_2O_2 in salt solutions up to 10 M. However, the ionic strength in rainwater is too low to impose the "salting-in" effect (Li et al., 2019). Therefore, we need to seek other explanations. In addition, the gas-phase H_2O_2 level at the ground after a shower was higher than before the shower, revealing that raindrops could release H_2O_2 into the gas phase at the ground (Hua et al., 2008). This opens up new possibilities for explaining the high level of H_2O_2 in rainwater. Nevertheless, the falling of raindrops is a complex process that involves several uncertainties, so observation studies are needed to quantitatively explain the high concentration in rainwater.

The measured level of H_2O_2 in aerosol particles was much higher than the theoretical value for gas-aerosol partitioning, by two orders of magnitude (Hasson and Paulson, 2003; Arellanes et al. 2006). In previous studies, it was confirmed that considerable H_2O_2 could be produced from redox reactions in aerosols, like transition metals (Charrier et al., 2014). However, it is noticeable that continuous redox reactions are assisted by available reductants, so it is impossible for ambient aerosols to generate H_2O_2 from transition metals without an additional reduced agent (Shen et al., 2011). Recently, numerous studies have reported the decomposition of organic peroxides in the aerosol phase (Krapf et al., 2016; Riva et al., 2017). Li et al. (2016) suggested that the decomposition/hydrolysis of organic peroxides on secondary organic aerosol particles could substantially raise the level of H_2O_2. Qiu et al. (2019) proposed that α-hydroxyalkyl-hydroperoxides could be easily decomposed into H_2O_2 within 2 h in ≥ 10 % water mixtures. However, the quantitative measurement of organic peroxides is difficult because of their instability (Zhao et al., 2018). The decomposition of labile organic peroxides should be studied in atmospheric fine particles ($PM_{2.5}$) in heavily polluted areas. In addition, H_2O_2 is easily to adsorbed onto aerosol particles, its heterogeneous uptake should also be considered. Hence, a quantitative evaluation of sources other than gas-phase partitioning is needed with the support of field measurements.

Compared to gas-phase H_2O_2, it is challenging to quantitatively understand the chemistry of H_2O_2 in the liquid and aerosol phases. To the best of our knowledge, this is the first study to measure H_2O_2 in gas-liquid or gas-aerosol phases simultaneously

https://doi.org/10.5194/acp-2020-34
Preprint. Discussion started: 20 January 2020


Atmospheric Chemistry and Physics Discussions

in a heavily polluted area, e.g., Beijing, providing a good opportunity to better understand the partitioning of H_2O_2 in different phases. The objectives of this study are to explore the partitioning of H_2O_2 in the gas-liquid and gas-aerosol phases in the ambient atmosphere and to seek possible sources other than gas-phase partitioning that could increase H_2O_2 concentration in the liquid and aerosol phases.

2 Experimental

2.1 Measurement site

The online gas-phase measurement of peroxides was performed at the Peking University (PKU) site (39.99° N 116.30° E), situated in the northwest of urban Beijing. The PKU site is a typical city site in a heavily polluted area in Beijing, with two main trunks of traffic to the east and south. The relative apparatuses were placed on the roof of a building that was ~ 26 m above ground level. In this study, we introduce two measurements at the PKU site: BJ-2018Summer (23 July−10 August 2018 and 25 August−11 September 2018) and BJ-2018Winter (21 December 2018−5 January 2019).

2.2 Measurement methods

2.2.1 Gas-phase peroxides

The concentrations of gas-phase peroxides were observed in both BJ-2018Summer and BJ-2018Winter using high performance liquid chromatography (HPLC, Agilent 1200, USA) with a time resolution of 21 min. The HPLC coupled with the post-column enzyme derivatization method could distinguish H_2O_2 from organic peroxides. This method is well established (Hua et al., 2008; He et al., 2010) and is only briefly described here. Ambient air was drawn into a glassy scrubbing coil at a flow rate of 2.7 standard L min^{-1}. H_3PO_4 solution (5×10^{-3} M) was added to the scrubbing coil at 0.2 mL min^{-1} to dissolve H_2O_2 from ambient air. The collection efficiency of H_2O_2 was validated to close to 100 %, while it was ~ 85 % for organic peroxides. Then, the mixture was injected into HPLC with the mobile phase (H_3PO_4, 5×10^{-3} M). Peroxides separated by the column reacted stoichiometrically with parahydroxyphenylacetic acid (PHPAA) under the Hemin catalyst, generating stable PHPAA dimers that were measured by a fluorescence detector. The peroxides were identified and quantified using standard samples, and the detection limit (DL) of the gas-phase H_2O_2 was about 10 pptv. The values below DL were replaced by DL divided by the square root of two (the same hereafter). The gas-phase samples during BJ-2018Summer were used for the partitioning analysis in the gas-liquid phase, while the data of BJ-2018Winter were used to study the partitioning in the gas-aerosol phase.

2.2.2 Liquid-phase peroxides

Rain samples were collected by a custom-built glass funnel and used for the analysis of liquid-phase peroxides in BJ-2018Summer. During the observation period, the collection of rain samples was well organized depending on the intensity, amount, and duration of the rain. Because the peroxides were easy to break down, the collected rain samples were preserved

https://doi.org/10.5194/acp-2020-34
Preprint. Discussion started: 20 January 2020


Atmospheric Chemistry and Physics Discussions

in brown vials at 4 ℃ until they could be analysed with HPLC within 6 h. The subsequent detection method for the liquid-phase peroxides was the same as for the gas-phase peroxides. In all, we collected 60 rain samples during seven rain episodes, and the DL of the liquid-phase H_2O_2 was about 8 nM. The specific dates of the rain events in chronological order were 24 July, 25 July, 5 August, 6 August, 8 August, 30 August and 2 September.

2.2.3 Aerosol-phase peroxides

Aerosol-phase samples were gathered on Teflon filters (Whatman™, 47 mm diameter and 2 μm pore size) using a four-channel filter sampler (Wuhan Tianhong TH-16A, China) at 16.7 standard L min^{-1} during BJ-2018Winter. Teflon filters were supported by stainless steel filter holders during the 11.5 h sampling time. We immediately disposed of two Teflon filters for the analysis of peroxides and total peroxides (TPO_S), and the remaining filters were kept under refrigeration at −18 ℃ for subsequent component analysis. For analysing the aerosol-phase peroxides, the Teflon filters were immediately extracted with 10 mL H_3PO_4 in conical flasks and placed on a shaker to be blended thoroughly at 4 ℃ and 180 rpm for 15 min. Then, the extracted solution was measured with HPLC within 40 min. The extracted solution was also used for the measurement of TPOs using the iodometric spectrophotometric method, which could measure H_2O_2 as well as organic peroxides. (Nozaki, 1946; Banerjee and Budke, 1964). After the oxygen in the extracted solution was blown off by bubbling with nitrogen for 5 min, 250 μL potassium iodide solution (KI, 0.75 M) was added to the solution to react with TPOs in the dark for 12−24 h (Reactions R1 and R2). The reaction product I_3^- ion could be detected using UV/Vis spectrophotometry (Beijing PERSEE TU-1810, China) at the wavelength of 420 nm. A total of 31 aerosol-phase samples were analysed, and the DL of aerosol-phase H_2O_2 was close to 0.24 ng m^{-3} (0.006 ng μg^{-1}).

To avoid the matrix influence on samples (i.e., Teflon filters and the H_3PO_4 solution), we measured the concentration of blank samples in every extraction. The level of H_2O_2 in three-quarters of the blank samples was equal to 0 μM, and the concentration of H_2O_2 in the remnant blank samples was below 10 % of that in the ambient air samples. To prevent the matrix influence, we deducted the background values of the samples. In addition, to ensure that the measured H_2O_2 was attributed to aerosols collected on Teflon filters, we performed experiments to demonstrate that the physical adsorption on clean Teflon filters without aerosols was responsible for 15 % of the measured H_2O_2 in samples. The details are available in Fig. S1 in the Supplement. In this study, we did not correct the physical adsorption to avoid introducing new errors.

$$3I^- + H_2O_2 + 2H^+ \rightarrow I_3^- + 2H_2O \quad \text{(R1)}$$

$$R_1OOR_2 + 3I^- + 2H^+ \rightarrow I_3^- + R_1OH + R_2OH \quad \text{(R2)}$$

2.2.4 Other components and meteorological parameters

Water-soluble cations (Na^+, NH_4^+, K^+, Mg^{2+}, and Ca^{2+}) as well as anions (Cl^-, NO_3^-, and SO_4^{2-}) were measured with ion chromatography (IC, Dionex ICS2000 and ICS2500, USA). Transition metal elements deposited on Teflon filters were measured with inductively coupled plasma mass spectrometry (ICP-MS, Bruker aurora M90, Germany). The mass

https://doi.org/10.5194/acp-2020-34
Preprint. Discussion started: 20 January 2020


Atmospheric Chemistry and Physics Discussions

concentration of $PM_{2.5}$ was measured with a TEOM 1400a analyser. Meteorological parameters (temperature, relative humidity, and wind speed) and major trace gases (O_3, SO_2, NO-NO_2-NO_x and CO) were monitored simultaneously using a series of commercial instruments (Met One Instruments Inc., Thermo 49i, 43i, 42i, and 48i).

2.3 Estimation of effective partitioning coefficients

To estimate the effective partitioning coefficients, we could use the field-derived Henry's law constant for the gas-liquid phase and the gas-aerosol partitioning coefficient for the gas-aerosol phase (Pankow, 1994), which are estimated according to Eqs. (1)–(4).

$$H_A^t = 8.4 \times 10^4\ M\ atm^{-1} \quad (1)$$

$$H_A^m = \frac{C_{aq}^m}{C_g^m} \quad (2)$$

$$K_P^t = \frac{RT_W f_{om}}{10^6 \overline{MW_{OM}} \zeta p_L^0} \quad (3)$$

$$K_P^m = \frac{C_p^m}{C_g^m C_{om}} \quad (4)$$

In Eqs. (1) and (2), C_{aq}^m is the liquid-phase level of H_2O_2, M; C_g^m is the partial pressure of the gas-phase H_2O_2, atm; and H_A^t and H_A^m are the theoretical values in pure water and the effective field-derived Henry's law constant, respectively, M atm^{-1} (Sander et al., 2011). The average temperature during rainfall in summer (T_S) was 298 ± 2 K (mean ± standard deviation, the same hereafter). In Eq. (3), K_P^t is the theoretical value of the gas-aerosol partitioning coefficient, m^3 μg^{-1}; $\overline{MW_{OM}}$ is the estimated average molecular weight of organic compounds, 200 g mol^{-1} (Williams et al., 2010; Xie et al., 2014); p_L^0 is the vapour pressure of pure H_2O_2 at the specified temperature, calculated by the extrapolation of the Antoine equation (Maass and Hiebert, 1924; Baum et al., 1997); ζ is the activity coefficient of H_2O_2, assumed to be unity (Pankow, 1994); f_{om} is the weight fraction of H_2O_2 absorbing on aerosols, also set to unity (Liang et al., 1997; Shen et al., 2018); R is the ideal gas constant, 8.2×10^{-5} atm m^3 mol^{-1} K^{-1}; and T_W is the mean temperature during BJ-2018Winter, 270 ± 4 K for the whole observation period, 272 ± 4 K for day-time, and 269 ± 4 K for night-time. In Eq. (4), C_p^m and C_g^m are the concentrations of H_2O_2 in the aerosol and gas phases, respectively, μg m^{-3}; C_{om} is the organic matter concentration, referring to the mass concentration of $PM_{2.5}$, μg m^{-3}; and K_P^m is the effective field-derived gas-aerosol partitioning coefficient, m^3 μg^{-1}.

3 Results and discussion

3.1 Gas-liquid phase partitioning

3.1.1 Gas- and liquid-phase H_2O_2 in summer

The concentration of gas-phase H_2O_2 was statistically counted to be 0.30 ± 0.26 parts per billion by volume (ppbv) for the

https://doi.org/10.5194/acp-2020-34
Preprint. Discussion started: 20 January 2020


Atmospheric Chemistry and Physics Discussions

seven rainfalls (Fig. S2a in the Supplement) and 0.53 ± 0.77 ppbv for the entire BJ-2018Summer. Compared with the theoretical liquid-phase H_2O_2 value in pure water with 25.20 μM, the level of measured H_2O_2 in the liquid phase was 44.12 ± 26.49 μM (3.19−139.95 μM), as shown in Fig. S2b. The detailed values of the peroxides in the gas and liquid phases are shown in Table S1. Based on Eq. (2), the effective field-derived Henry's law constant, H_A^m, averaged 2.1×10^5 M atm^{-1} in rain samples, which was two and a half times the theoretical pure-water Henry's law constant, H_A^t, at 8.4×10^4 M atm^{-1} and 298 ± 2 K. The analysis result shows that 88 % of the measured liquid-phase H_2O_2 came from gas-phase partitioning, while 12 % of H_2O_2 was from other sources. In 23 % of the total rain samples, H_A^m was less than H_A^t, indicating that these samples followed Henry's law (Fig. 1). In the remaining 77 % of the samples, the measured liquid-phase H_2O_2 was larger than the predicted values (Fig. 1), and the difference averaged 28 μM with a maximum of 71 μM. Further, 54 % of liquid-phase H_2O_2 in these samples was produced from other sources than gas-phase partitioning.

To explain the difference between H_A^m and H_A^t, we should rule out the effect of pressure, pH, and T_S on H_A^t. First, to our knowledge, the influence of pressure on H_A^t can usually be neglected under conditions of less than 1 atm (Lind and Kok, 1986). Also, H_A^t of H_2O_2 is independent of pH in the range of 4−7 (Xu et al., 2012); therefore, the present study does not consider the influence of pressure and pH on H_A^t. The temperature during BJ-2018Summer can be divided into three ranges: 294−296 K, 297−299 K, and 300−306 K. The percentage of samples in these three temperature ranges were 25 %, 63 %, and 12 %, respectively, and the ratios of H_A^m to H_A^t in the same temperature ranges were 1.4, 2.6, and 4.5, respectively. The maximum value of H_A^t in the range 294−306 K was 1.2×10^5 M atm^{-1}, while H_A^m reached 4.2×10^5 M atm^{-1} at the 90th percentile. This suggests that the influence of T_S on H_A^m was negligible. The nonlinear relationship between H_A^m and T_S, shown in Fig. S3, also indicates that T_S plays an unimportant role in determining H_A^m. Thus, other explanations need to be explored to understand the difference between H_A^m and H_A^t.

3.1.2 Process of raindrops falling

The solubility of H_2O_2 in clouds was larger than that in the ground rainwater. There is a negative dependence of the solubility on temperature (Huang and Chen, 2010), which allows for the possibility of mass transfer of H_2O_2 from rainwater to the surrounding air when falling. Let us assume that the gas-phase H_2O_2 concentration is homogeneous and the rain droplet size remains constant during its fall. The diameter of the raindrops (D_P) is mainly distributed in the range of 0.05–2.50 mm. Calculations were performed for typical droplet diameters at 0.1 mm, 0.5 mm, 1.0 mm and 2.0 mm. The height of the precipitation cloud base during summer time in north China was almost less than 2000 m (Shang et al., 2012). As a result, we assumed the fall distance to be 500 m, 1000 m, 1500 m, and 2000 m, respectively, which are same to previous studies (Adamowicz, 1979; Levine and Schwartz, 1982). In the process of falling, it is necessary to consider the mass transfer resistance in the gas and liquid phases. However, it could be that the shear force generated on the raindrop surface when it fell improved the mixing rate in the droplet significantly; therefore, the liquid-phase mass transfer resistance was negligible (Pruppacher and Klett, 1997; Elperin and Fominykh, 2005). Thus, the overall mass transfer resistance reduced to the mass

https://doi.org/10.5194/acp-2020-34
Preprint. Discussion started: 20 January 2020


Atmospheric Chemistry and Physics Discussions

transfer resistance in the gas phase.

Here, we first discuss residual H_2O_2 in raindrops after a fall from a height of 1000 m. The temperature in clouds (T_S^c) was estimated to be 292 K, 6 K lower than the ground. H_A^t in pure water at 292 K is 1.4 × 10^5 M atm^{-1} (Sander et al., 2011). Provided that the droplet started at equilibrium with the cloud atmosphere, the initial level of liquid-phase H_2O_2 before falling (C_{aq}^0) was 42.87 μM. However, the equilibrium was broken when the raindrops fell as the ambient temperature increased. The mass transfer coefficient in the gas phase (k_g) can be calculated by Eqs. (S1)−(S4) in the Supplement (Levine and Schwartz, 1982; Kumar, 1985). The concentration of H_2O_2 in the droplet at the ground (C_{aq}^d) can be estimated by Eq. (S5). The results are presented in Table 1, which shows us that the large droplet has a small mass transfer coefficient. As a result, the liquid-phase H_2O_2 in the large raindrops is more slowly released into the air. C_{aq}^d of the droplet diameter at 2.0 mm was close to C_{aq}^0, while C_{aq}^d at 0.1 mm approximated the theoretical level of liquid-phase H_2O_2 in pure water at 298 K, as indicated by Fig. 2. The results show that the effect of residual H_2O_2 in large raindrops on ground rainwater levels could be of great importance. Next, we investigated the influence of different fall distances on C_{aq}^d. The decreasing temperature at increasing fall distances caused larger H_A^t and C_{aq}^0 in clouds, and C_{aq}^d also increased. The wide gap of C_{aq}^d between different fall distances is more visible for the large droplet, as seen in Fig. 2. Based on the above analysis, the residual H_2O_2 in large raindrops can increase the H_2O_2 level in rainwater to a maximum of 48.81 μM at a fall distance of 2000 m, which explains to a large extent the difference between the measured and predicted levels of H_2O_2 in rainwater.

Based on the rain intensity, seven rain events during BJ-2018 Summer could be divided into three types, as shown in Table S2 in the Supplement. Rain events in types I, II, and III have rain intensities < 1 mm h^{-1}, 1−10 mm h^{-1}, and > 10 mm h^{-1}, respectively. The larger the diameter of raindrops, the greater the rain intensity (Kumar., 1985). According to the above relationship between the diameter of raindrops and level of liquid-phase H_2O_2 in the ground rainwater, the difference between the measured and predicted liquid-phase H_2O_2 levels should be greater as the hourly rain intensity increased. We found that the differences between C_{aq}^m and C_{aq}^t increased during the rain periods on 25 July and 5 August, which the maximum hourly rain intensities were more than 10 mm h^{-1}. Because it is difficult for the liquid-phase H_2O_2 in heavy rains to diffuse into the gas phase, much H_2O_2 may be retained in the ground rainwater, which could well represent the level of H_2O_2 in cloud water.

During the rain episode on 1−2 September 2018, the concentration of gas-phase H_2O_2 decreased over time. However, there was a sudden rise from 0.47 ppbv at 1:03 local time (LT) to 0.66 ppbv at 1:46 LT, which subsequently dropped to 0.38 ppbv over time (Fig. 3a). Surprisingly, the difference between the measured and predicted levels of liquid-phase H_2O_2 reached a low value in the meantime, indicating that the increase in gas-phase H_2O_2 was due to the release of H_2O_2 from raindrops that could contain high levels of H_2O_2, as presented in Fig. 3b. Compared with Fig. S4 in the Supplement, which describes the relationship between rain intensity and time, the rain intensity simultaneously dropped to 3.51 mm h^{-1} from 6.35 mm h^{-1}, consequently decreasing the diameter of the raindrops (Kumar, 1985) and increasing the mass transfer of H_2O_2 from rainwater to the gas phase. Provided that 20 μM H_2O_2 in rainwater was released into ambient air, the increase in the gas-phase H_2O_2 level was 0.24 ppbv, which was in accordance with the sudden rise during 1:03−1:46 LT on 1−2 September 2018.

https://doi.org/10.5194/acp-2020-34
Preprint. Discussion started: 20 January 2020


Atmospheric Chemistry and Physics Discussions

The above analysis is based on the assumption that the gas-phase H_2O_2 concentration is uniform. However, the distribution of gas-phase H_2O_2 at different heights may be complicated. We could use the average level of H_2O_2 in rainwater at the ground to estimate the concentrations of H_2O_2 in cloud water (C_{aq}^c) and the nearby atmosphere (C_g^c), as presented in Table 2. Assuming the simplest case, D_P is 1.0 mm, the fall distance is 1000 m, and H_2O_2 in the gas phase and rainwater at the ground is 0.30 ppbv and 44.12 μM at 298 K. Considering the release of H_2O_2 from raindrops into ambient air during the falling process, the level of H_2O_2 in cloud water should be 47 μM. Based on Henry's law, the surrounding gas-phase H_2O_2 may be 0.33 ppbv, a little higher than that at the ground. When the fall distance is 500 m, 1500 m, and 2000 m, H_2O_2 in cloud water should be 46 μM, 49 μM, and 51 μM, respectively, and H_2O_2 in nearby ambient air could be 0.41 ppbv, 0.26 ppbv, and 0.21 ppbv, respectively.

3.2 Gas-aerosol phase partitioning

3.2.1 Gas- and aerosol-phase H_2O_2 in winter

From 21 December 2018 to 5 January 2019, the gas-phase H_2O_2 level was 24.08 ± 28.83 parts per trillion by volume (pptv), as shown in Fig. S5a in the Supplement. We eluted Teflon filters with H_3PO_4 solution and measured the level of H_2O_2 in the extracted solution to calculate the aerosol-phase H_2O_2 concentration. The mass concentration of aerosol-phase H_2O_2 and the normalized concentration to aerosol mass were 2.22 ± 1.49 ng m^{-3} (< 0.24−6.75 ng m^{-3}) and 0.093 ± 0.085 ng μg^{-1} (< 0.006−0.409 ng μg^{-1}), respectively. The mean concentration of the aerosol-phase H_2O_2 at night-time (0.107 ± 0.102 ng μg^{-1}) was higher than that at day-time (0.079 ± 0.066 ng μg^{-1}), as presented in Fig. S5b. The measured level of H_2O_2 in aerosols was much higher than the predicted value using Pankow's absorptive partitioning theory, which suggested that the aerosols collected on the filter existed under non-equilibrium conditions and may arise from sources other than gas-phase partitioning in the aerosol phase. Based on Eqs. (3) and (4), K_P^m was equal to $3.8 \times 10^{-3} \pm 4.8 \times 10^{-3}$ m^3 μg^{-1} at 270 ± 4 K, which was four orders of magnitude more than K_P^t, 2.8×10^{-7} m^3 μg^{-1}. The effects of parameter variation (e.g., T_W, ζ, $\overline{MW_{OM}}$, and f_{om}) could not account for the large discrepancy between K_P^m and K_P^t (Shen et al., 2018), and other factors are needed to explain the difference. In terms of the proportion of theoretical to measured concentrations, the partitioning of gas-phase H_2O_2 into aerosols could be neglected, and nearly all of aerosol-phase H_2O_2 was generated from other reactions besides gas-phase partitioning.

The level of aerosol-phase H_2O_2 in the present study was lower than those reported in previous studies (Table S3), which may be due to the extraction method, the extraction time, reduced substance levels, and aerosol pH values, as shown in the Supplement. Assuming a molecular weight of 300 g mol^{-1} (Docherty et al., 2005; Epstein et al., 2014), the level of TPOs averaged 10.26 ± 6.38 ng μg^{-1} (2.08−28.75 ng μg^{-1}). It was calculated that H_2O_2 took up a small fraction of TPOs, equal to 8 ± 6 % in molar concentration ratio, which indicated that organic peroxides accounted for a large proportion of peroxides, and could play important roles in the formation of $PM_{2.5}$ and secondary organic aerosols.

https://doi.org/10.5194/acp-2020-34
Preprint. Discussion started: 20 January 2020


Atmospheric Chemistry and Physics Discussions

3.2.2 Factor analysis

Figure 4 shows that the concentration of aerosol-phase H_2O_2 is dependent on RH, first increasing and then decreasing as RH increases. The variation of H_2O_2 with RH was the result of competition between production and consumption processes. Here, the production process refers to either process that favours increasing the level of aerosol-phase H_2O_2, while the consumption process denotes those processes consuming aerosol-phase H_2O_2. In the first stage, the higher RH could accelerate the heterogeneous uptake of H_2O_2 onto aerosols and enhance the level of aerosol-phase H_2O_2 (Pradhan et al., 2010; Shiraiwa et al., 2011; Zhao et al., 2013; Slade and Knopf, 2015). The level of H_2O_2 is negatively associated with RH in the subsequent stage, ascribed to the much more rapid consumption of H_2O_2 due to its oxidizing the reduced substances, such as SO_2 into SO_4^{2-}, on polluted days.

We considered a heavy haze episode, from 2 January to 3 January 2019, as an example to explain in detail the important contribution of aerosol-phase H_2O_2 to SO_4^{2-} growth on polluted days. The $PM_{2.5}$ mass concentration of the severe haze event was up to 201.20 μg m^{-3}. The estimation of aerosol water content is shown in the Supplement. Based on the measured H_2O_2, the reaction rate (RR) and sulfate formation rate (SFR) averaged about 3.03 × 10^{-3} μmol m^{-3} h^{-1} and 0.29 μg m^{-3} h^{-1} (Table S4), respectively. The detailed calculation process is provided in the Supplement. In addition, the growth rate of SO_4^{2-} calculated by the measured data was 0.51 μg m^{-3} h^{-1}, accounting for about 9 % of the observed formation of $PM_{2.5}$. H_2O_2 oxidation pathway contributed about 57 % of the measured growth of SO_4^{2-} in $PM_{2.5}$. This result strongly suggests that the aerosol-phase H_2O_2 indeed acts as the important oxidant in the formation of sulfate and plays significant roles in the rapid growth of $PM_{2.5}$ during pollution events.

Next, we consider that the consumption rate of aerosol-phase H_2O_2 increases with an increase of RH. It is suggested that larger levels of SO_4^{2-} and $PM_{2.5}$ are often accompanied by higher RH. In Fig. 5, the reverse curve between aerosol-phase SO_4^{2-} and H_2O_2 got steeper with the formation of SO_4^{2-}, indicating that the rate of consumption of H_2O_2 on polluted days was much higher than that on clear days, which could offer proof of rapid H_2O_2 consumption with increasing RH. In addition, the level of H_2O_2 in the aerosol phase exhibited a negative correlation with $PM_{2.5}$ mass concentration, as shown in Fig. 5. In other words, the aerosol-phase H_2O_2 concentration was lower on polluted days than on clear days, which further demonstrates that the removal rate of H_2O_2 by oxidizing SO_2 into SO_4^{2-} exceeded the production rate during pollution events with high RH.

3.2.3 Heterogenous uptake of H_2O_2

In addition to the factors that influencing the aerosol-phase H_2O_2 concentration, there are other physical and chemical reactions besides gas-phase partitioning that increase the level of aerosol-phase H_2O_2, e.g., heterogeneous uptake of H_2O_2 on aerosols. Previous studies have shown that heterogeneous uptake of H_2O_2 is positively related with RH. High RH is beneficial to the mass transfer of H_2O_2 from the gas phase to the aerosol phase, accelerating the reaction between H_2O_2 and reduced compositions of aerosols, thus contributing to the more heterogenous uptake of H_2O_2 (Huang et al., 2015; Wu et al., 2015). To quantitatively evaluate the importance of the heterogeneous uptake of H_2O_2 on aerosols to the aerosol-phase H_2O_2, we

https://doi.org/10.5194/acp-2020-34
Preprint. Discussion started: 20 January 2020


Atmospheric Chemistry and Physics Discussions

calculated the average of total heterogeneous uptake during the sampling process based on Eqs. (S6)−(S11) in the Supplement. Details about each parameter are introduced in Table 3. Compared with the averaged measured content of aerosol-phase H_2O_2 ($[X]_p^m$, 0.057 ng μg^{-1}), the total heterogeneous uptake of H_2O_2 ($[X]_p^{t,h}$) averaged 0.049 ng μg^{-1}, indicating that heterogeneous uptake of H_2O_2 could account for 86 % of the measured level of H_2O_2 in the aerosol phase.

3.2.4 Decomposition of organic peroxides

It was found that the concentration of H_2O_2 in the extracted solution first increased rapidly, then reached peaks at distinct hours that depended on the particular sample, and finally gradually declined over time. However, interestingly, there was large sample-to-sample variation, with samples classifiable into three types in terms of the change trend and evolution duration (Fig. 6 and Table 4). The third type (Fig. 6c) occurs when H_2O_2 level exhibits a steady decline from 0.03 μM without a growth stage within 13 h, and this was the case with samples 5 and 6 on a slightly polluted day on 2 January 2019. Samples 1 and 2 on 29 December 2018 during clear days belonged to the first type (Fig. 6a), in which H_2O_2 rapidly grew within 5 h and subsequently decreased at a slow rate over 25 h. The evolution trends of H_2O_2 in the second type (samples 3 and 4, Fig. 6b) during clear days from 31 December 2018 to 1 January 2019 were similar to the those of the first type, except H_2O_2 approached its peak at about 40 h over the whole analysis process lasting for about 300 h.

To seek the reasons for the elevated level of H_2O_2 in the extracted solution, we compared the ratio of the maximum (C_{max}) to initial (C_0) H_2O_2 concentration in the extracted solution with the molar concentration ratio of the aerosol-phase TPOs to H_2O_2 and found that the ratios of C_{max}/C_0 and TPOs/H_2O_2 were the same order of magnitude for the first and second types, as exhibited in Table S5 in the Supplement. This result provided evidence that part of aerosol-phase H_2O_2 originated from the decomposition/hydrolysis of organic peroxides, as described in earlier studies (Wang et al., 2011; Li et al., 2016). In the second type, the concentration of TPOs normalized to aerosol mass reached a maximum, indicating that the second type has more TPOs sources and consequently causing higher TPOs/H_2O_2 and C_{max}/C_0 ratios compared with the first type. Furthermore, the aerosol surface is semi-liquid or liquid under high RH (Liu et al., 2017), which provides reaction sites for the decomposition/hydrolysis of aerosol-phase organic peroxides. Aerosol-phase organic peroxides could decompose into H_2O_2 when the particle aerosols were collected (Zhao et al., 2018). The rates of the decomposition/hydrolysis of organic peroxides to H_2O_2 in the first and second types were 0.14 ng μg^{-1} and 3.65 ng μg^{-1}, respectively.

The three types of samples were in accordance with the growth process of $PM_{2.5}$. According to meteorological parameters and trace gases data (Table S6 in the Supplement), static weather conditions gradually formed and were accompanied by lower wind speed, lower ozone level, higher RH, and higher gaseous pollutants. The mass concentration of $PM_{2.5}$ increased from 13.45 μg m^{-3} to 63.11 μg m^{-3}. In addition, the mass concentration of TPOs showed a rising trend. But the level of TPOs normalized to aerosol mass increased at first and decreased afterwards due to the rapid growth of $PM_{2.5}$. Because of the consumption of reactive TPOs which formed SO_4^{2-} during polluted days, the rest of the TPOs were stable organic peroxides that could not easily decompose into H_2O_2, e.g., peroxide esters (ROOR). The ratio of TPOs/H_2O_2 in the third type, collected

https://doi.org/10.5194/acp-2020-34
Preprint. Discussion started: 20 January 2020


Atmospheric Chemistry and Physics Discussions

on a slightly polluted day, was close to that in the second type on clear days, but a rising trend of H_2O_2 in the extracted solution could not be observed. It was calculated that the ratios of decomposable TPOs to total TPOs for the three types were 29 %, 98 %, and 0 %, respectively.

Recently, it was reported that organic peroxides account for a large proportion of secondary organic aerosol (SOA) mass, varying widely from less than 20 % to 60 % (Docherty et al., 2005; Li et al., 2016; Gong et al., 2018). Peroxy radicals also paly important parts in the formation of highly oxygenated molecules (HOMs) via an autoxidation mechanism, which can form aerosols without sulfuric acid nucleation (Kirkby et al., 2016). The thermal decomposition of peroxide-containing SOAs and HOMs contribute to the formation of aerosol-phase H_2O_2 (Krapf et al., 2016). A similar phenomenon was also found by Li et al. (2016), in which the decomposition/hydrolysis of organic peroxides sustainably generated H_2O_2 accompanied by the attenuation of TPOs in the extracted solution, and about 18 % of gaseous organic peoxides experienced the heterogeneous decomposition on aerosols into H_2O_2. The decomposable organic peroxides are often peroxycarboxylic acids (PCAs, e.g., peroxyacetic acid, PAA; peroxyformic acid, PFA) and α-hydroxyalkyl-hydroperoxides (α-HAHPs, e.g., hydroxymethyl hydroperoxide, HMHP). Based on previous studies and the evolution trend of the three types in this study, we speculate that PCAs and α-HAHPs accounted for a large proportion of the first and second types, while ROOR played a large part in the third type, as shown in Table 4.

3.3 Source and sink of H_2O_2 in rainwater and aerosol

To provide support for the sources suggested above, we analysed the source and sink of liquid- and aerosol-phase H_2O_2 in rainwater and aerosols. In this study, the measured level of H_2O_2 was the concentration after partial or complete reaction with reduced substances, such as SO_2 onto the particles. The contribution of different additional sources in the liquid and aerosol phases should be estimated compared with the important sink.

The liquid-phase H_2O_2 level was the result of the combined effect between sources (gas-phase partitioning and residual H_2O_2 in raindrops) and sinks (reaction with S(IV) and the decomposition of H_2O_2). Based on the foregoing description, the dissolved gas-phase H_2O_2 in rainwater was 25.20 μM at 298 K. The residual H_2O_2 in raindrops could enhance the level of liquid-phase H_2O_2 by up to 48.81 μM, based on Henry's law. The largest removal pathway was the consumption by its oxidizing dissolved SO_2 into sulfate. Given that the major oxidants to sulfate formation were only H_2O_2 and O_3 (Penkett et al., 1979; Chandler et al., 1988), the proportions of the H_2O_2 oxidation pathway to the overall, calculated by Eqs. (S12) and (S13) in the Supplement, were 92 % at pH 5 and 11 % at pH 6, respectively. The average of sulfate concentration in rainwater measured 31.95 μM, and the H_2O_2 oxidation pathway contributed to the sulfate with 29 μM at pH 5 and 4 μM at pH 6, which was the consumption level of H_2O_2. In addition, the decomposition of H_2O_2 during 6 h storage time before analysis was 6 μM (Li et al., 2016). To summarize, the concentration of liquid-phase H_2O_2 was supposed to have its maximum at 64.01 μM, a bit lower than the 90th percentile of the measured level (67.85 μM). This could be considered to achieve the approximate balance between sources and sinks in the liquid-phase H_2O_2. Consequently, the residual H_2O_2 in raindrops could explain the difference between H_A^m

https://doi.org/10.5194/acp-2020-34
Preprint. Discussion started: 20 January 2020


Atmospheric Chemistry and Physics Discussions

and H_A^t.

In terms of the sources and sinks for aerosol-phase H_2O_2, the main removal pathway was the consumption of H_2O_2 to sulfate formation, similar to the sink of H_2O_2 in the liquid phase. The average mass concentrations of $PM_{2.5}$ and aerosol-phase SO_4^{2-} were 39.21 μg m^{-3} and 2.20 μg m^{-3}, respectively. The mass concentration ratio of SO_4^{2-} to $PM_{2.5}$ was 6 % in this study, which was lower than previous studies (Ho et al., 2016; Shao et al., 2018). The discrepancy may be accounted by the decreased ratio of SO_4^{2-} to $PM_{2.5}$ due to SO_2 emissions control in recent years, as shown in the Supplement. Accordingly, the H_2O_2 oxidation pathway accounted for 57 % of the sulfate formation in a typical haze event on 2−3 January 2019, and the consumption of aerosol-phase H_2O_2 caused by sulfate formation maximized at 11.33 ng μg^{-1}. In this study, the maximum amount of H_2O_2 formed by the decomposition/hydrolysis of organic peroxides was close to 3.65 ng μg^{-1}, accounting for 32 % of the H_2O_2 formation in the aerosol phase. The heterogeneous uptake of H_2O_2 on aerosols had a minor contribution to the aerosol-phase H_2O_2, and the proportion was less than 0.5 %. The sources could not achieve a balance with the consumption of the aerosol-phase H_2O_2. Provided that the γ value could reach 10^{-3} (Wang et al., 2016), the amount of heterogeneous uptake could reach 0.49 ng μg^{-1}. However, this still does not bridge the difference between sinks and sources. In our view, there are a couple of possible explanations for the difference. First, we estimated the contribution of the H_2O_2 oxidation pathway to sulfate formation during the entire measurement period based on the contribution of high-pollution days, which may overestimate the sink for the aerosol-phase H_2O_2. Provided that the contribution ratio was 20 % on clear days, the sink for aerosol-phase H_2O_2 to sulfate formation could be 3.97 ng μg^{-1}, which was in general accordance with the sources for aerosol-phase H_2O_2. Second, the inverse dependence of the γ value on the gas-phase H_2O_2 concentration was not considered, and the γ value could have been underestimated when the level of gas-phase H_2O_2 in winter was much lower (Romanias et al., 2012; Romanias et al., 2013). Third, there may be missing sources in aerosol-phase H_2O_2. There are possibly some potential sources that are not completely understood, such as the heterogeneous uptake of HO_2 on aerosols forming aerosol-phase H_2O_2 (Liang et al., 2013) and so on. Based on the above analysis, sources and sinks of H_2O_2 in the liquid phase could achieve balance, while the formation of H_2O_2 from the decomposition/hydrolysis of aerosol-phase organic peroxides and the heterogeneous uptake of H_2O_2 could not offset the consumption of H_2O_2 in the aerosol phase. Two-thirds of the total aerosol-phase H_2O_2 formation failed to be explained by the two possible sources. Field measurements and laboratory experiments are urgently needed to further study the possible reasons and search for other potential sources of aerosol-phase H_2O_2.

4 Conclusions

In this study, we simultaneously measured H_2O_2 concentrations in gas and rainwater in summer as well as in the gas and aerosol phases ($PM_{2.5}$) in winter over urban Beijing. For the investigated seven rain episodes, the average H_A^m was 2.1×10^5 M atm^{-1}, which was 2.5 times greater than H_A^t at 298 ± 2 K. The liquid-phase concentration of H_2O_2 averaged 44.12 ± 26.49 μM. In 77 % of the rain samples, the liquid-phase H_2O_2 level was much larger than the predicted values estimated for pure water using Henry's law. We found that 12 % of measured H_2O_2 in all samples and 54 % of measured H_2O_2 in those samples that did not

https://doi.org/10.5194/acp-2020-34
Preprint. Discussion started: 20 January 2020


Atmospheric Chemistry and Physics Discussions

follow Henry's law were from residual H_2O_2 in raindrops. With an increase in raindrops diameter and fall distance, the proportion of the additional source of liquid-phase H_2O_2 gradually increased. Furthermore, the source and sink in rainwater could achieve a balance.

For the measured $PM_{2.5}$ aerosol samples, a similar phenomenon was observed between the measured and predicted levels of H_2O_2 in the aerosol phase, but the difference was much higher than that in the liquid phase. K_P^m averaged 3.8×10^{-3} m^3 μg^{-1}, which was four orders of magnitude higher than K_P^t at 270 ± 4 K. The aerosol-phase concentration of H_2O_2 normalized to the aerosol mass averaged 0.093 ± 0.085 ng μg^{-1}. Aerosol-phase H_2O_2 level was associated with relative humidity, increasing before decreasing, which resulted from the competition between the formation and consumption of H_2O_2. The decomposition/hydrolysis of organic peroxides produced the elevated aerosol-phase H_2O_2 at a maximum rate of 3.65 ng μg^{-1}, which was responsible for 32 % of the formation of aerosol-phase H_2O_2. The heterogeneous uptake of H_2O_2 played a minor role in increasing the H_2O_2 level in the aerosol phase, and the proportion was less than 0.5 %. There are many uncertainties in the decomposition/hydrolysis of organic peroxides in this study, and laboratory simulation studies are needed to quantify the roles of different organic peroxides in the decomposition process. Aerosol-phase H_2O_2 in this study cannot reach source and sink equilibrium, and there are missing sources of aerosol-phase H_2O_2. Due to a lack of substantial severe haze events with high RH in this study, the source and sink mentioned in the aerosol-phase H_2O_2 need to be further verified.

Our study has provided direct evidence to prove that the partitioning of H_2O_2 between the gas-liquid and gas-aerosol phases not only follows thermodynamic equilibrium but is affected by certain physical and chemical reactions. The effective field-derived Henry's law constant and gas-aerosol partitioning coefficient should be accepted to better predict the measured liquid- and aerosol-phase H_2O_2 concentrations, which would be beneficial to correctly calculating the contribution of H_2O_2 to the fast formation of SO_4^{2-} and $PM_{2.5}$ during pollution episodes. More laboratory experiments and field measurements are urgently needed to improve our understanding of the partitioning of peroxides in different phases in the atmosphere.

Data availability. The data are accessible by contacting the corresponding author (zmchen@pku.edu.cn).

Author contributions. In the framework of BJ-2018Summer and BJ-2018Winter measurements, ZC and XX designed the study. XX carried out all peroxide measurements used in this study, analysed the data, and wrote the paper. ZC helped interpret the results, guided the writing, and modified the manuscript. YG contributed to the methods of analysing aerosol-phase hydrogen peroxides and total peroxides. HS helped interpret data and modify the paper. SC provided the data for the meteorological parameters, trace gases and $PM_{2.5}$ mass concentrations. All authors discussed the results and contributed to the final paper.

Competing interests. The authors declare that they have no conflict of interest.

Acknowledgements. This work was funded by the National Key Research and Development Program of China (Grants 2016YFC0202704), National Research Program for Key Issues in Air Pollution Control (Grants DQGG0103) and the National

https://doi.org/10.5194/acp-2020-34
Preprint. Discussion started: 20 January 2020

Natural Science Foundation of China (Grants 21477002).

https://doi.org/10.5194/acp-2020-34
Preprint. Discussion started: 20 January 2020

Atmospheric Chemistry and Physics Discussions

References

Adamowicz, R. F.: A model for the reversible washout of sulfur-dioxide, ammonia and carbon-dioxide from a polluted atmosphere and the production of sulfates in raindrops, Atmos. Environ., 13, 105−121, https://doi.org/10.1016/0004-6981(79)90250-6, 1979.

Arellanes, C., Paulson, S. E., Fine, P. M., and Sioutas, C.: Exceeding of Henry's law by hydrogen peroxide associated with urban aerosols, Environ. Sci. Technol., 40, 4859−4866, https://doi.org/10.1021/es0513786, 2006.

Banerjee, D. K. and Budke, C. C.: Spectrophotometric determination of traces of peroxides in organic solvents, Anal. Chem., 36, 792−796, https://doi.org/10.1021/ac60210a027, 1964.

Baum, E. J.: Chemical property estimation: theory and application, CRC Press Inc., Grand Valley State university, the United States of America, 1997.

Campbell, S. J., Stevanovic, S., Miljevic, B., Bottle, S. E., Ristovski, Z., and Kalberer, M.: Quantification of particle-bound organic radicals in secondary organic aerosol, Environ. Sci. Technol., 53, 6729−6737, https://doi.org/10.1021/acs.est.9b00825, 2019.

Chandler, A. S., Choularton, T. W., Dollard, G. J., Eggleton, A. E. J., Gay, M. J., Hill, T. A., Jones, B. M. R., Tyler, B. J., Bandy, B. J., and Penkett, S. A.: Measurements of H_2O_2 and SO_2 in clouds and estimates of their reaction rate, Nature, 336, 562−565, https://doi.org/10.1038/336562a0, 1988.

Charrier, J. G., McFall, A. S., Richards-Henderson, N. K., and Anastasio, C.: Hydrogen peroxide formation in a surrogate lung fluid by transition metals and quinones present in particulate matter, Environ. Sci. Technol., 48, 7010−7017, https://doi.org/10.1021/es501011w, 2014.

Chung, M. Y., Muthana, S., Paluyo, R. N., and Hasson, A. S.: Measurements of effective Henry's law constants for hydrogen peroxide in concentrated salt solutions, Atmos. Environ., 39, 2981−2989, https://doi.org/10.1016/j.atmosenv.2005.01.025, 2005.

Crowley, J. N., Pouvesle, N., Phillips, G. J., Axinte, R., Fischer, H., Petäjä, T., Nölscher, A., Williams, J., Hens, K., Harder, H., Martinez-Harder, M., Novelli, A., Kubistin, D., Bohn, B., and Lelieveld, J.: Insights into HO_x and RO_x chemistry in the boreal forest via measurement of peroxyacetic acid, peroxyacetic nitric anhydride (PAN) and hydrogen peroxide, Atmos. Chem. Phys., 18, 13457−13479, https://doi.org/10.5194/acp-18-13457-2018, 2018.

Docherty, K. S., Wu, W., Lim, Y. B., and Ziemann, P. J.: Contributions of organic peroxides to secondary aerosol formed from reactions of monoterpenes with O_3, Environ. Sci. Technol., 39, 4049−4059, https://doi.org/10.1021/es050228s, 2005.

Elperin, T. and Fominykh, A.: Conjugate mass transfer during gas absorption by falling liquid droplet with internal circulation, Atmos. Environ., 39, 4575−4582, https://doi.org/10.1016/j.atmosenv.2005.04.005, 2005.

Epstein, S. A., Blair, S. L., and Nizkorodov, S. A.: Direct photolysis of α-pinene ozonolysis secondary organic aerosol: effect on particle mass and peroxide content, Environ. Sci. Technol., 48, 11251−11258, https://doi.org/10.1021/es502350u, 2014.

Gong, Y. W., Chen, Z. M., and Li, H.: The oxidation regime and SOA composition in limonene ozonolysis: roles of different

double bonds, radicals, and water, Atmos. Chem. Phys., 18, 15105−15123, https://doi.org/10.5194/acp-18-15105-2018, 2018.

Gunn, R. and Kinzer, G. D.: The terminal velocity of fall for water droplets in stagnant air, J. Meteorol., 6, 243−248, https://doi.org/10.1175/1520-0469(1949)006<0243:TTVOFF>2.0.CO;2, 1949.

Gurgueira, S. A., Lawrence, J., Coull, B., Murthy, G. G. K., and González-Flecha, B.: Rapid increases in the steady-state concentration of reactive oxygen species in the lungs and heart after particulate air pollution inhalation, Environ. Health Perspect., 110, 749−755, https://doi.org/10.1289/ehp.02110749, 2002.

Hasson, A. S. and Paulson, S. E.: An investigation of the relationship between gas-phase and aerosol-borne hydroperoxides in urban air, J. Aerosol. Sci., 34, 459−468, https://doi.org/10.1016/S0021-8502(03)00002-8, 2003.

He, S. Z., Chen, Z. M., Zhang, X., Zhao, Y., Huang, D. M., Zhao, J. N., Zhu, T., Hu, M., and Zeng, L. M.: Measurement of atmospheric hydrogen peroxide and organic peroxides in Beijing before and during the 2008 Olympic Games: chemical and physical factors influencing their concentrations, J. Geophys. Res.-Atmos., 115, D17307, https://doi.org/10.1029/2009JD013544, 2010.

Ho, K. F., Ho, S. S. H., Huang, R. J., Chuang, H. C., Cao, J. J., Han, Y. M., Lui, K. H., Ning, Z., Chuang, K. J., Cheng, T. J., Lee, S. C., Hu, D., Wang, B., and Zhang, R. J.: Chemical composition and bioreactivity of $PM_{2.5}$ during 2013 haze events in China, Atmos. Environ., 126, 162−170, https://doi.org/10.1016/j.atmosenv.2015.11.055, 2016.

Hua, W., Chen, Z. M., Jie, C. Y., Kondo, Y., Hofzumahaus, A., Takegawa, N., Chang, C. C., Lu, K. D., Miyazaki, Y., Kita, K., Wang, H. L., Zhang, Y. H., and Hu, M.: Atmospheric hydrogen peroxide and organic hydroperoxides during PRIDE-PRD'06, China: their concentration, formation mechanism and contribution to secondary aerosols, Atmos. Chem. Phys., 8, 6755−6773, https://doi.org/10.5194/acp-8-6755-2008, 2008.

Huang, D. M. and Chen, Z. M.: Reinvestigation of the Henry's law constant for hydrogen peroxide with temperature and acidity variation, J. Environ. Sci., 22, 570−574, http://doi.org/10.1016/S1001-0742(09)60147-9, 2010.

Huang, L. B., Zhao, Y., Li, H., and Chen, Z. M.: Kinetics of heterogeneous reaction of sulfur dioxide on authentic mineral dust: effects of relative humidity and hydrogen peroxide, Environ. Sci. Technol., 49, 10797−10805, https://doi.org/10.1021/acs.est.5b03930, 2015.

Kirkby, J., Duplissy, J., Sengupta, K., Frege, C., Gordon, H., Williamson, C., Heinritzi, M., Simon, M., Yan, C., Almeida, J., Trostl, J., Nieminen, T., Ortega, I. K., Wagner, R., Adamov, A., Amorim, A., Bernhammer, A. K., Bianchi, F., Breitenlechner, M., Brilke, S., Chen, X. M., Craven, J., Dias, A., Ehrhart, S., Flagan, R. C., Franchin, A., Fuchs, C., Guida, R., Hakala, J., Hoyle, C. R., Jokinen, T., Junninen, H., Kangasluoma, J., Kim, J., Krapf, M., Kurten, A., Laaksonen, A., Lehtipalo, K., Makhmutov, V., Mathot, S., Molteni, U., Onnela, A., Perakyla, O., Piel, F., Petaja, T., Praplan, A. P., Pringle, K., Rap, A., Richards, N. A. D., Riipinen, I., Rissanen, M. P., Rondo, L., Sarnela, N., Schobesberger, S., Scott, C. E., Seinfeld, J. H., Sipila, M., Steiner, G., Stozhkov, Y., Stratmann, F., Tome, A., Virtanen, A., Vogel, A. L., Wagner, A. C., Wagner, P. E., Weingartner, E., Wimmer, D., Winkler, P. M., Ye, P. L., Zhang, X., Hansel, A., Dommen, J., Donahue, N. M., Worsnop, D. R., Baltensperger, U., Kulmala, M., Carslaw, K. S., and Curtius, J.: Ion-induced nucleation of pure biogenic particles, Nature,

533, 521−526, https://doi.org/10.1038/nature17953, 2016.

Krapf, M., Haddad, I. E., Bruns, E. A., Molteni, U., Daellenbach, K. R., Prévôt, A. S. H., Baltensperger, U., and Dommen, J.: Labile peroxides in secondary organic aerosol, Chem, 1, 603−616, https://doi.org/10.1016/j.chempr.2016.09.007, 2016.

Kumar, S.: An Eulerian model for scavenging of pollutants by raindrops, Atmos. Environ., 19, 769−778, https://doi.org/10.1016/0004-6981(85)90065-4, 1985.

Lee, M. H., Heikes, B. G., and O'Sullivan, D. W.: Hydrogen peroxide and organic hydroperoxide in the troposphere: a review, Atmos. Environ., 34, 3475−3494, https://doi.org/10.1016/S1352-2310(99)00432-X, 2000.

Levine, S. Z. and Schwartz, S. E.: In-cloud and below-cloud scavenging of nitric-acid vapor, Atmos. Environ., 16, 1725−1734, https://doi.org/10.1016/0004-6981(82)90266-9, 1982.

Li, H., Chen, Z. M., Huang, L. B., and Huang, D.: Organic peroxides' gas-particle partitioning and rapid heterogeneous decomposition on secondary organic aerosol, Atmos. Chem. Phys., 16, 1837−1848, https://doi.org/10.5194/acp-16-1837-2016, 2016.

Li, T., Wang, Z., Wang, Y., Wu, C., Liang, Y., Xia, M., Yu, C., Yun, H., Wang, W., Wang, Y., Guo, J., Herrmann, H., and Wang, T.: Chemical characteristics of cloud water and the impacts on aerosol properties at a subtropical mountain site in Hong Kong, Atmos. Chem. Phys. Discuss., https://doi.org/10.5194/acp-2019-481, in review, 2019.

Liang, C. K., Pankow, J. F., Odum, J. R., and Seinfeld, J. H.: Gas/particle partitioning of semivolatile organic compounds to model inorganic, organic, and ambient smog aerosols, Environ. Sci. Technol., 31, 3086−3092, https://doi.org/10.1021/es9702529, 1997.

Liang, H., Chen, Z. M., Huang, D., Zhao, Y., and Li, Z. Y.: Impacts of aerosols on the chemistry of atmospheric trace gases: a case study of peroxides and HO_2 radicals, Atmos. Chem. Phys., 13, 11259−11276, https://doi.org/10.5194/acp-13-11259-2013, 2013.

Lind, J. A., and Kok, G. L.: Henry's law determinations for aqueous solutions of hydrogen peroxide, methylhydroperoxide, and peroxyacetic acid, J. Geophys. Res.-Atmos., 91, 7889−7895, https://doi.org/10.1029/JD091iD07p07889, 1986.

Liu, T. Y., Clegg, S. L., and Abbatt, J. P. D.: Fast oxidation of sulfur dioxide by hydrogen peroxide in deliquesced aerosol particles, Proc. Natl. Acad. Sci. U. S. A., 201916401, https://doi.org/10.1073/pnas.1916401117, 2020.

Liu, Y. C., Wu, Z. J., Wang, Y., Xiao, Y., Gu, F. T., Zheng, J., Tan, T. Y., Shang, D. J., Wu, Y. S., Zeng, L. M., Hu, M., Bateman, A. P., and Martin, S. T.: Submicrometer particles are in the liquid state during heavy haze episodes in the urban atmosphere of Beijing, China, Environ. Sci. Technol. Lett., 4, 427−432, https://doi.org/10.1021/acs.estlett.7b00352, 2017.

Maass, O. and Hiebert, P. G.: The properties of pure hydrogen peroxide. v. vapor pressure, J. Am. Chem. Soc., 46, 2693−2700, https://doi.org/10.1021/ja01677a012, 1924.

Nozaki, K.: Iodometric method of analysis for organic peroxides, Ind. Eng. Chem., 18, 583−583, https://doi.org/10.1021/i560157a020, 1946.

O'Sullivan, D. W., Lee, M., Noone, B. C., and Heikes, B. G.: Henry's law constant determinations for hydrogen peroxide, methyl hydroperoxide, hydroxymethyl hydroperoxide, ethyl hydroperoxide, and peroxyacetic acid, J. Phys. Chem., 100,

3241−3247, https://doi.org/10.1021/jp951168n, 1996.

Pankow, J. F.: An absorption model of gas-particle partitioning of organic compounds in the atmosphere, Atmos. Environ., 28, 185−188, https://doi.org/10.1016/1352-2310(94)90093-0, 1994.

Penkett, S. A., Jones, B. M. R., Brich, K. A., and Eggleton, A. E. J.: The importance of atmospheric ozone and hydrogen peroxide in oxidising sulphur dioxide in cloud and rainwater, Atmos. Environ., 13, 123−137, https://doi.org/10.1016/j.atmosenv.2007.10.065, 1979.

Pradhan, M., Kyriakou, G., Archibald, A. T., Papageorgiou, A. C., Kalberer, M., and Lambert, R. M.: Heterogeneous uptake of gaseous hydrogen peroxide by Gobi and Saharan dust aerosols: a potential missing sink for H_2O_2 in the troposphere, Atmos. Chem. Phys., 10, 7127−7136, https://doi.org/10.5194/acp-10-7127-2010, 2010.

Pruppacher, H. R. and Klett, J. D.: Microphysics of clouds and precipitation, Kluwer Academic Publishers, Dordrecht, Holland, 1997.

Qin, M. R., Chen, Z. M., Shen, H. Q., Li, H., Wu, H. H., and Wang, Y.: Impacts of heterogeneous reactions to atmospheric peroxides: observations and budget analysis study, Atmos. Environ., 183, 144−153, https://doi.org/10.1016/j.atmosenv.2018.04.005, 2018.

Qiu, J., Ishizuka, S., Tonokura, K., Colussi, A. J., and Enami, S.: Water dramatically accelerates the decomposition of α-hydroxyalkyl-hydroperoxides in aerosol particles, J. Phys. Chem. Lett., 10, 5748−5755, https://doi.org/10.1021/acs.jpclett.9b01953, 2019.

Reeves, C. E. and Penkett, S. A.: Measurements of peroxides and what they tell us, Chem. Rev., 103, 5199−5218, https://doi.org/10.1021/cr0205053, 2003.

Riva, M., Budisulistiorini, S. H., Zhang, Z. F., Gold, A., Thornton, J. A., Turpin, B. J., and Surratt, J. D.: Multiphase reactivity of gaseous hydroperoxide oligomers produced from isoprene ozonolysis in the presence of acidified aerosols, Atmos. Environ., 152, 314−322, https://doi.org10.1016/j.atmosenv.2016.12.040, 2017.

Romanias, M. N., El Zein, A., and Bedjanian, Y.: Heterogeneous interaction of H_2O_2 with TiO_2 surface under dark and UV light irradiation conditions, J. Phys. Chem. A, 116, 8191−8200, https://doi.org/10.1021/jp305366v, 2012.

Romanias, M. N., El Zein, A., and Bedjanian, Y.: Uptake of hydrogen peroxide on the surface of Al_2O_3 and Fe_2O_3, Atmos. Environ., 77, 1−8, https://doi.org/10.1016/j.atmosenv.2013.04.065, 2013.

Sander, S. P., Abbatt, J., Barker, J. R., Burkholder, J. B., Friedl, R. R., Golden, D. M., Huie, R. E., Kolb, C. E., Kurylo, M. J., Moortgat, G. K., Orkin, V. L., and Wine, P. H.: Chemical kinetics and photochemical data for use in atmospheric studies, Evaluation No. 17, JPL Publication 10-6, Jet Propulsion Laboratory, Pasadena, http://jpldataeval.jpl.nasa.gov, 2011.

Seinfeld, J. H. and Pandis S. N.: Atmospheric chemistry and physics: from air pollution to climate change, A Wiley-Interscience Publication, New Jersey, the United States of America, 2006.

Shang, B., Zhou, Y. Q., Liu, J. C., and Huang, Y. M.: Comparing vertical structure of precipitation cloud and non-precipitation cloud using Cloudsat, J. Appl. Meteorol. Clim., 23, 1−9, https://doi.org/10.3969/j.issn.1001-7313.2012.01.001, 2012.

Shao, P. Y., Tian, H. Z., Sun, Y. J., Liu, H. J., Wu, B. B., Liu, S. H., Liu, X. Y., Wu, Y. M., Liang, W. Z., Wang, Y., Gao, J. J.,

Xue, Y. F., Bai, X. X., Liu, W., Lin, S. M., and Hu, G. Z.: Characterizing remarkable changes of severe haze events and chemical compositions in multi-size airborne particles (PM_1, $PM_{2.5}$ and PM_{10}) from January 2013 to 2016–2017 winter in Beijing, China, Atmos. Environ., 189, 133–144, https://doi.org/10.1016/j.atmosenv.2018.06.038, 2018.

Shen, H., Barakat, A. I., and Anastasio, C.: Generation of hydrogen peroxide from San Joaquin Valley particles in a cell-free solution, Atmos. Chem. Phys., 11, 753–765, https://doi.org/10.5194/acp-11-753-2011, 2011.

Shen, H. Q., Chen, Z. M., Li, H., Qian, X., Qin, X., and Shi, W. X.: Gas-particle partitioning of carbonyl compounds in the ambient atmosphere, Environ. Sci. Technol., 52, 10997–11006, https://doi.org/10.1021/acs.est.8b01882, 2018.

Shiraiwa, M., Ammann, M., Koop, T., and Pöschl, U.: Gas uptake and chemical aging of semisolid organic aerosol particles, Proc. Natl. Acad. Sci. U. S. A., 108, 11003–11008, https://doi.org/10.1073/pnas.1103045108, 2011.

Slade, J. H. and Knopf, D. A.: Multiphase OH oxidation kinetics of organic aerosol: the role of particle phase state and relative humidity, Geophys. Res. Lett., 41, 5297–5306, https://doi.org/10.1002/2014GL060582, 2015.

Stein, A. F. and Saylor, R. D.: Sensitivities of sulfate aerosol formation and oxidation pathways on the chemical mechanism employed in simulations, Atmos. Chem. Phys., 12, 8567–8574, https://doi.org/10.5194/acp-12-8567-2012, 2012.

Tong, H., Arangio, A. M., Lakey, P. S. J., Berkemeier, T., Liu, F., Kampf, C. J., Brune, W. H., Pöschl, U., and Shiraiwa, M.: Hydroxyl radicals from secondary organic aerosol decomposition in water, Atmos. Chem. Phys., 16, 1761–1771, https://doi.org/10.5194/acp-16-1761-2016, 2016.

Wang, Y., Chen, Z. M., Wu, Q. Q., Liang, H., Huang, L. B., Li, H., Lu, K. D., Wu, Y. S., Dong, H. B., Zeng, L. M., and Zhang, Y. H.: Observation of atmospheric peroxides during Wangdu Campaign 2014 at a rural site in the North China Plain, Atmos. Chem. Phys., 16, 10985–11000, https://doi.org/10.5194/acp-16-10985-2016, 2016.

Wang, Y., Kim, H., and Paulson, S. E.: Hydrogen peroxide generation from α- and β-pinene and toluene secondary organic aerosols, Atmos. Environ., 45, 3149–3156, https://doi.org/10.1016/j.atmosenv.2011.02.060, 2011.

Williams, B. J., Goldstein, A. H., Kreisberg, N. M., and Hering, S. V.: In situ measurements of gas/particle-phase transitions for atmospheric semivolatile organic compounds, Proc. Natl. Acad. Sci. U. S. A., 107, 6676–6681, https://doi.org/10.1073/pnas.0911858107, 2010.

Wu, Q. Q., Huang, L. B., Liang, H., Zhao, Y., Huang, D., and Chen, Z. M.: Heterogeneous reaction of peroxyacetic acid and hydrogen peroxide on ambient aerosol particles under dry and humid conditions: kinetics, mechanism and implications, Atmos. Chem. Phys., 15, 6851–6866, https://doi.org/10.5194/acp-15-6851-2015, 2015.

Xie, M. J., Hannigan, M. P., and Barsanti, K. C.: Gas/particle partitioning of n-alkanes, PAHs and oxygenated PAHs in urban Denver, Atmos. Environ., 95, 355–362, https://doi.org/10.1016/j.atmosenv.2014.06.056, 2014.

Xu, Z. F., Tang, Y., and Ji, J. P.: Chemical and strontium isotope characterization of rainwater in Beijing during the 2008 Olympic year, Atmos. Res., 107, 115–125, https://doi.org/10.1016/j.atmosres.2012.01.002, 2012.

Ye, C., Liu, P. F., Ma, Z. B., Xue, C. Y., Zhang, C. L., Zhang, Y. Y., Liu, J. F., Liu, C. T., Sun, X., and Mu, Y. J.: High H_2O_2 concentrations observed during haze periods during the winter in Beijing: importance of H_2O_2 oxidation in sulfate formation, Environ. Sci. Technol. Lett., 5, 757–763, https://doi.org/10.1021/acs.estlett.8b00579, 2018.

https://doi.org/10.5194/acp-2020-34
Preprint. Discussion started: 20 January 2020

Zhao, R., Kenseth, C. M., Huang, Y., Dalleska, N. F., and Seinfeld, J. H.: Iodometry-assisted liquid chromatography electrospray ionization mass spectrometry for analysis of organic peroxides: an application to atmospheric secondary organic aerosol, Environ. Sci. Technol., 52, 2108−2117, https://doi.org/10.1021/acs.est.7b04863, 2018.

Zhao, Y., Chen, Z. M., Shen, X. L., and Huang, D.: Heterogeneous reactions of gaseous hydrogen peroxide on pristine and acidic gas-processed calcium carbonate particles: effects of relative humidity and surface coverage of coating, Atmos. Environ., 67, 63−72, https://doi.org/10.1016/j.atmosenv.2012.10.055, 2013.

Zhao, Y., Chen, Z. M., Shen, X. L., and Zhang, X.: Kinetics and mechanisms of heterogeneous reaction of gaseous hydrogen peroxide on mineral oxide particles, Environ. Sci. Technol., 45, 3317−3324, https://doi.org/10.1021/es104107c, 2011.

https://doi.org/10.5194/acp-2020-34
Preprint. Discussion started: 20 January 2020

Atmospheric Chemistry and Physics Discussions

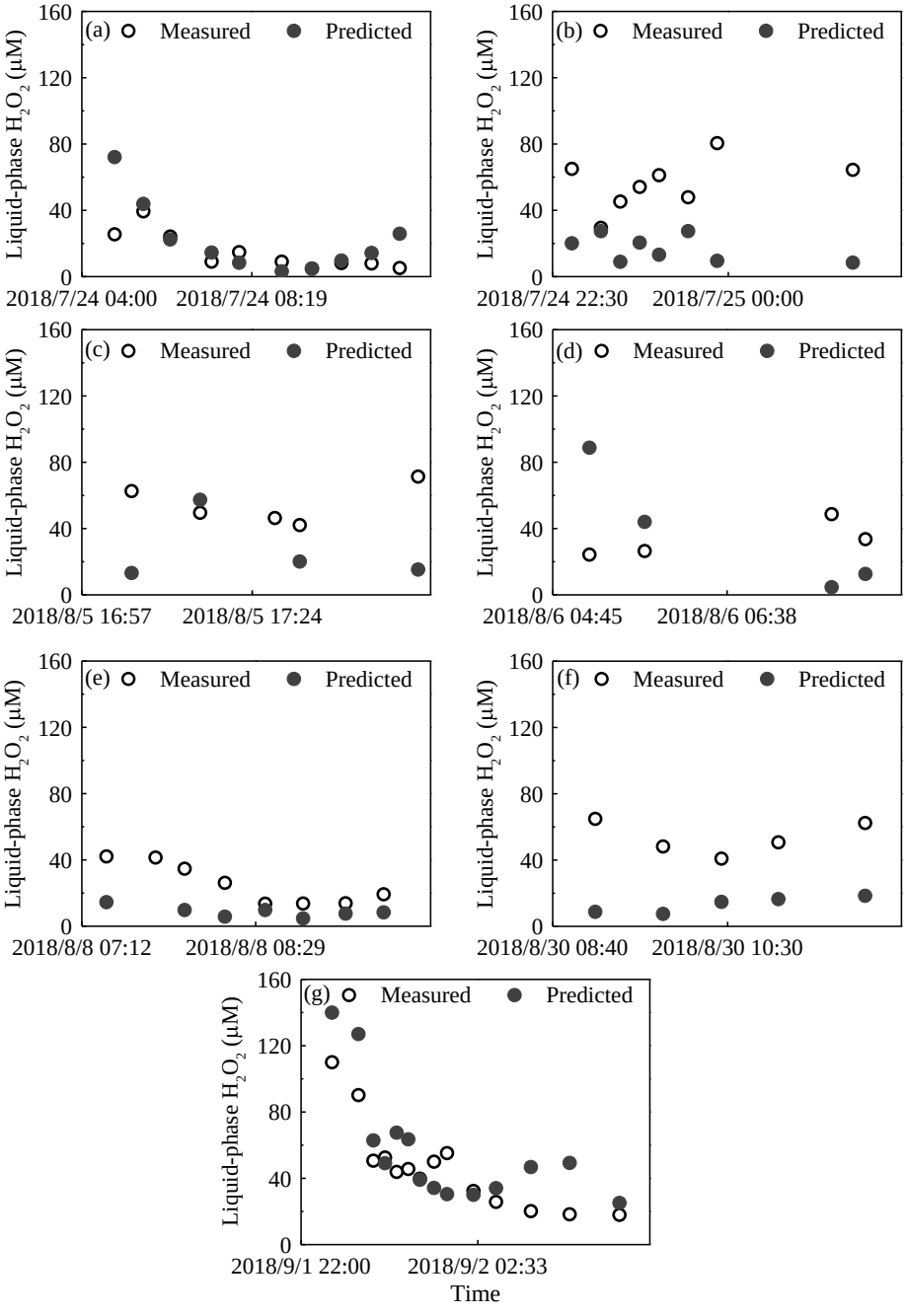

585 **Figure 1: Time profiles of measured and predicted concentrations of H_2O_2 from seven rain episodes. The seven rainfall events are listed in chronological order: (a) 24 July, (b) 25 July, (c) 5 August, (d) 6 August, (e) 8 August, (f) 30 August, and (g) 2 September.**

https://doi.org/10.5194/acp-2020-34
Preprint. Discussion started: 20 January 2020

Atmospheric Chemistry and Physics Discussions

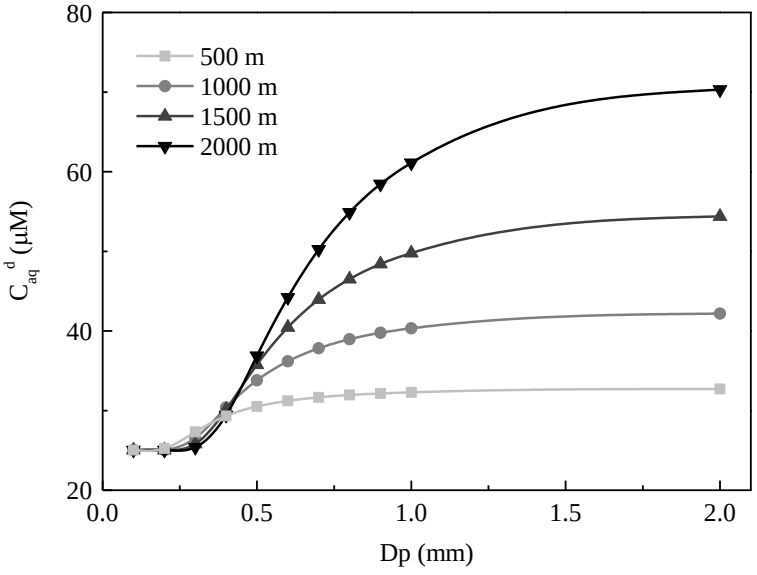

Figure 2: The dependence of the concentration of H_2O_2 in the ground raindrops (C_{aq}^{d}) on the diameter of the raindrops. The light grey, grey, dark grey, and black lines denote fall distances of 500 m, 1000 m, 1500 m, and 2000 m, respectively.

590

https://doi.org/10.5194/acp-2020-34
Preprint. Discussion started: 20 January 2020

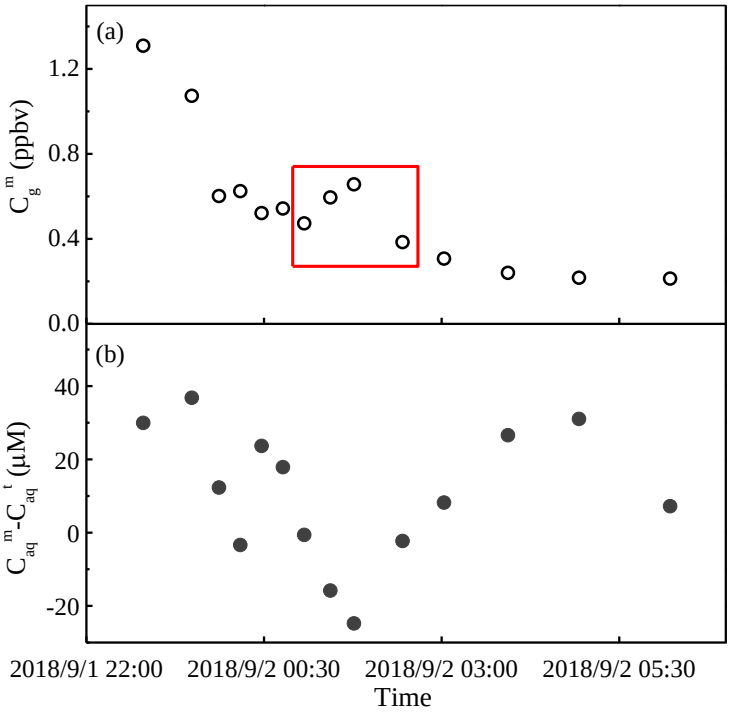

Figure 3: The measured and predicted H_2O_2 levels in a rain event on 1−2 September 2018. (a) Gas-phase H_2O_2 (C_g^m). (b) The difference between measured (C_{aq}^m) and theoretical (C_{aq}^t) levels of H_2O_2 in the liquid phase. The red box indicates a sudden rise in gas-phase H_2O_2.

595

https://doi.org/10.5194/acp-2020-34
Preprint. Discussion started: 20 January 2020

Atmospheric Chemistry and Physics Discussions

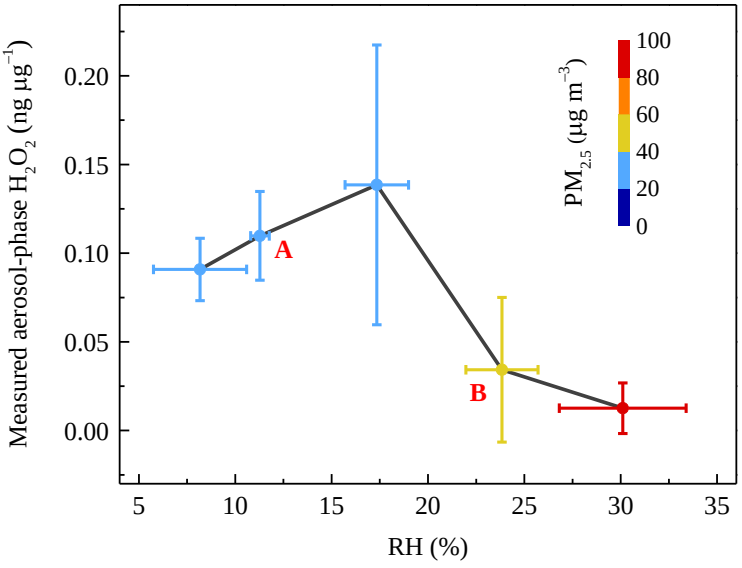

Figure 4: The relationship between measured aerosol-phase H_2O_2 level and relative humidity. Coloured circles denote the mass concentration of $PM_{2.5}$. The vertical error bars represent the standard deviations of aerosol-phase H_2O_2 concentration in every RH range bin.

600

https://doi.org/10.5194/acp-2020-34
Preprint. Discussion started: 20 January 2020

Atmospheric Chemistry and Physics Discussions

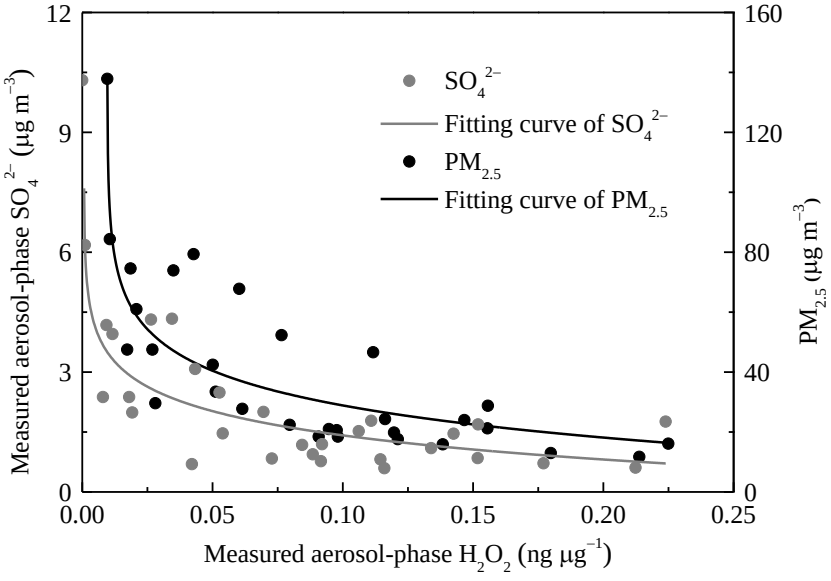

Figure 5: The negative dependence of the measured concentrations of aerosol-phase SO_4^{2-} and $PM_{2.5}$ on H_2O_2. The grey and black lines are the logarithmic fits for SO_4^{2-} level in aerosols and the $PM_{2.5}$ mass concentration, respectively.

605

https://doi.org/10.5194/acp-2020-34
Preprint. Discussion started: 20 January 2020

Atmospheric Chemistry and Physics Discussions

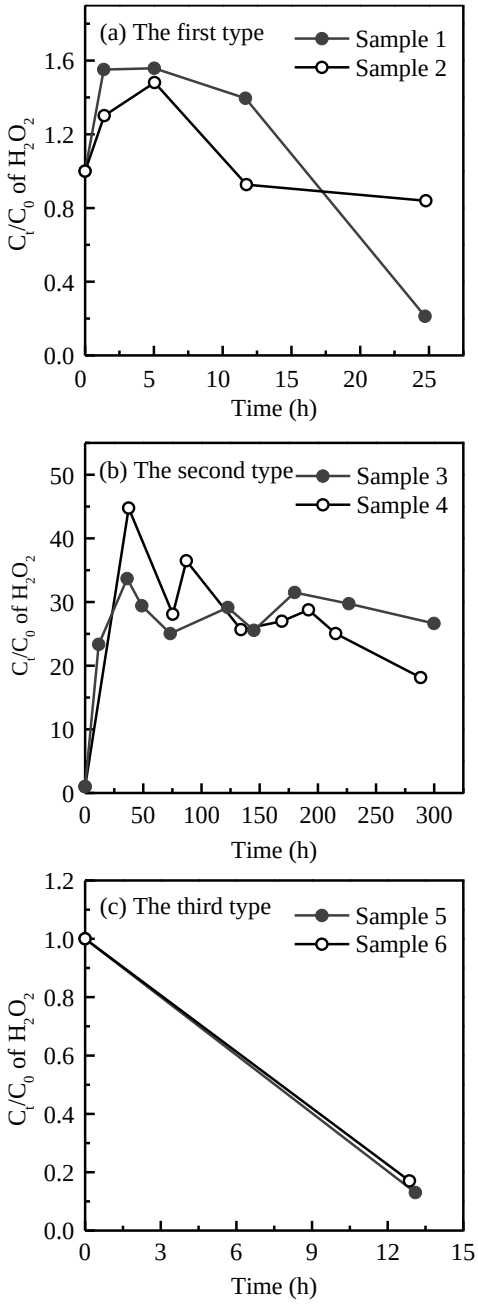

Figure 6: Time profiles of aerosol-phase H_2O_2 evolution in the extracted solution. (a) The first type: samples 1 and 2 were collected on 29 December 2018. (b) The second type: samples 3 and 4 were gathered on 31 December 2018−1 January 2019. (c) The third type: samples 5 and 6 were collected on 2 January 2019. C_t and C_0 denote molar concentrations of H_2O_2 in the extracted solution at time=t and time =0.

https://doi.org/10.5194/acp-2020-34
Preprint. Discussion started: 20 January 2020

Atmospheric Chemistry and Physics Discussions

Table 1: Calculating the level of H_2O_2 in the ground raindrops (C_{aq}^{d}) with different diameters from a height of 1000 m[a].

Parameters	D_P (mm)			
	0.1	0.5	1.0	2.0
u (m s^{-1})[b]	0.27	2.06	4.03	6.49
k_g (cm s^{-1})[c]	51.42	25.00	21.09	17.45
C_{aq}^{d} (μM)	25.03	33.81	40.34	42.18

[a] These parameters are calculated based on equations in Gunn and Kinzer (1949), Levine and Schwartz (1982), Kumar (1985), and Seinfeld and Pandis (2006).

615 [b] u is the terminal fall velocity of a raindrop.

[c] k_g is the mass transfer coefficient of H_2O_2 in the gas phase.

https://doi.org/10.5194/acp-2020-34
Preprint. Discussion started: 20 January 2020

Atmospheric Chemistry and Physics Discussions

Table 2: Estimates of the level of H_2O_2 in cloud water (C_{aq}^c) and the surrounding atmosphere (C_g^c) at different fall distances with a raindrop diameter of 1.0 mm.

Parameters	500 m	1000 m	1500 m	2000 m
T_S^c (K)[a]	295	292	289	286
H_A^t (M atm^{-1})	1.1×10^5	1.4×10^5	1.9×10^5	2.5×10^5
C_{aq}^c (μM)	45.64	47.27	49.04	50.95
C_g^c (ppbv)	0.41	0.33	0.26	0.21

[a] T_S^c is the temperature in cloud water.

https://doi.org/10.5194/acp-2020-34
Preprint. Discussion started: 20 January 2020

Atmospheric Chemistry and Physics Discussions

Table 3: Comparison between the theoretical heterogeneous uptake of H_2O_2 on aerosols ($[X]_p^{t,h}$) and the measured aerosol-phase H_2O_2 level ($[X]_p^m$)[a].

Parameters	T_W (K)	RH (%)	γ –[b]	A_{es} (cm^2)[c]	$[X]_g$ (molecules m^{-3})[d]	$[X]_p^{t,h}$ (ng μg^{-1})	$[X]_p^m$ (ng μg^{-1})
Averages	270	17.89	1.54×10^{-4}	9.00	6.65×10^{14}	0.049	0.057

[a] These parameters are calculated based on Wu et al. (2015).
[b] γ is the heterogeneous uptake coefficient, dimensionless.
[c] A_{es} is the effective reaction area of aerosols.
[d] $[X]_g$ is the concentration of gas-phase H_2O_2.

https://doi.org/10.5194/acp-2020-34
Preprint. Discussion started: 20 January 2020

Atmospheric Chemistry and Physics Discussions

Table 4: Comparison of the H_2O_2 evolution parameters in the extracted solution among the three types.

Parameters	First type	Second type	Third type
Peak time (h)	5	40	–
Decomposition rate of organic peroxides to H_2O_2 (ng μg^{-1})	0.14	3.65	–
C_{max}/C_0 of H_2O_2 (μM/μM)	1.52	39.22	1.00
TPOs/H_2O_2 (μM/μM)	5.25	40.06	47.59
Ratio of decomposable organic peroxides (%)	29	98	0
Possible organic peroxides	PCAs[a], α-HAHPs[b]	PCAs, α-HAHPs	ROOR[c]

[a] PCAs denote peroxycarboxylic acids, e.g., peroxyacetic acid, PAA; peroxyformic acid, PFA.
[b] α-HAHPs denote α-hydroxyalkyl-hydroperoxides, e.g., hydroxymethyl hydroperoxide, HMHP.
[c] ROOR denote peroxide esters.